Bioresource Technology 464 (2027) 135822

Contents lists available at ScienceDirect

Bioresource Technology

journal homepage: www.elsevier.com/locate/biortech

Effect of storage, aqueous ammonia soaking and hydrothermal pretreatments in anaerobic digestion of *Sparganium erectum* biomass

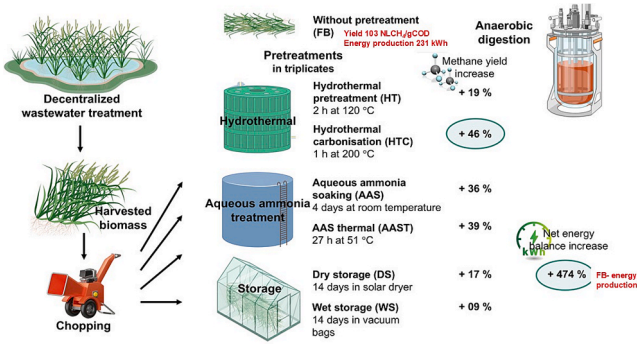
Pau Porras-Socias [a,b,c,d], Miriam Guivernau [a], Alexandre B. De Menezes [b], Carlos R. Gomes [c,d], C.Marisa R. Almeida [c], Ana Paula Mucha [c,d], Belén Fernández [a,*]

[a] IRTA Institute of Agrifood Research and Technology, SBS Program, Caldes de Montbui, Spain
[b] Microbiology, School of Biological and Chemical Sciences and Ryan Institute, University of Galway, Galway, Ireland
[c] CIIMAR, Interdisciplinary Centre of Marine and Environmental Research, University of Porto, Matosinhos, Portugal
[d] Faculty of Sciences, University of Porto, Porto, Portugal

HIGHLIGHTS

- Alkali and hydrothermal pretreatments modified biomass composition and structure.
- Dry/wet storage had minor changes on lignocellulose & organic matter content.
- Hydrothermal carbonization of biomass resulted in the highest methane yield.
- Dry storage was the most feasible option based on this study's economic analysis.
- Microbiome shifted under alkali and hydrothermal pre-treatments.

GRAPHICAL ABSTRACT



ARTICLE INFO

Keywords:
Emergent macrophyte
Methane
Lignocellulose
Biodegradability
Energy recovery

ABSTRACT

Sparganium erectum is a macrophyte whose use is very recent and offers a promising feedstock for biogas production. This study evaluates its methane yield after applying low and high-energy demand pretreatments (solar drying or ensiling, and aqueous ammonia soaking or hydrothermal treatment). These treatments are relatively easy to implement in existing biogas plants by using waste heat from the biogas engine or an aqueous ammonia solution recovered from the digestate. All pretreated biomasses exhibited higher methane yields than the untreated biomass (103 $NmLCH_4/gCOD$), reaching the hydrothermal carbonization at 200 °C the greatest increase (46 %). Drying altered slightly the biomass composition and structure, while alkali and hydrothermal pretreatments produced notable effects. Although all pretreatments enhanced the methane yield, less than 50 % of COD was converted, suggesting room for biodegradability improvement. At the microbiological level, only the alkaline pretreatment with ammonium caused a significant change in the population involved in anaerobic digestion, as well as a decrease in the abundance of taxa. These findings highlight the importance of pretreatments for the anaerobic digestion of macrophytes, where simple processes such as drying prove to be the most viable given its net energy gain obtained (474 %) compared to the obtained with untreated biomass (231 kWh).

* Corresponding author.
E-mail address: belen.fernandez@irta.cat (B. Fernández).

https://doi.org/10.1016/j.biortech.2026.135822
Received 19 May 2026; Received in revised form 17 August 2026; Accepted 7 September 2026
Available online 8 September 2026
0960-8524/© 2026 The Authors. Published by Elsevier Ltd. This is an open access article under the CC BY license (http://creativecommons.org/licenses/by/4.0/).

1. Introduction

The excessive natural growth of aquatic macrophytes poses a global problem disrupting human activities, requiring substantial resources for periodic removal to prevent flooding, avoid clogging, facilitate irrigation, control plagues, and enhance boat traffic and recreational activities (Thiemer et al., 2021). These plants can also constructed wetlands (CWs) use macrophytes to efficiently treat various pollutants in domestic, industrial, or agricultural effluents, improving the water quality (Fletcher et al., 2020) while generating significant biomass without competing with the human and husbandry food chain (Dotro et al., 2017). *Sparganium erectum*, prevalent specie in the *Sparganium* genus and commonly known as bur-reeds, is an emergent macrophyte that typically grows in shallow waters or very wet soils, found in various temperate regions of Europe, North Africa, Asia, North America, and Australia (Gottsberger, 2020). Although it has not been commonly employed so far, its prospects are driving recent attention since *S. erectum* also presents metal phytoextraction potential, making it a suitable candidate for CWs (Porras-Socias et al., 2024). A screening study in Germany showed that bur-reeds were the most abundant plants sampled and have a methane yield of 223 NmL CH_4/g VS (Moeller et al., 2018).

Current disposal methods (landfilling, incineration or composting) fail to realize the full resource potential of these abundant non-edible plants, while sustainable valorization strategies for biomass reuse are required (Kochi et al., 2020). Anaerobic digestion (AD) emerges as a promising cost-effective solution, converting macrophyte biomass into valuable bioenergy (Cinar et al., 2022). However, the efficient use of macrophytes in AD is constrained by their cell walls, composed of cross-linked polysaccharides (cellulose, hemicellulose and pectin), lignin and proteins, recalcitrant to chemical and/or microbial degradation even at high temperature (Ahmed et al., 2019; Alam et al., 2021; Moeller et al., 2018). Therefore, effective pretreatment strategies are essential to overcome this challenge and enhance the biodegradability of aquatic plants by improving the accessibility of cellulose and hemicellulose to microbial degradation by disrupting the lignin (Alam et al., 2021).

Comprehensive assessments of storage strategies and pretreatment technologies for *Sparganium erectum* remain scarce since research on macrophyte valorisation has mainly focused on species such as *Phragmites*, *Typha*, or *Egeria* (table S1 in E-supplementary materials). Furthermore, few studies have systematically compared low-cost preservation approaches, such as drying and ensiling, with more intensive alkaline and hydrothermal pretreatments within the same experimental framework. Pretreatments, classified as physical, chemical, physicochemical, or biological, vary in effectiveness across substrates. Mechanical methods (grinding or milling) reduce the particle size, incrementing the surface area and the microbial accessibility during AD (Abraham et al., 2020). Thermal drying facilitates waste management by reducing biomass volume and mass, saving costs in storage, handling, and transport, while also improves biogas production. Greenhouse solar drying offers a cost-effective and sustainable option (Papastefanakis et al., 2023). Another storage method is ensiling where the biomass is compacted and sealed under anaerobic conditions that promote lactic-acid fermentation: the pH drop enhances lignocellulosic digestibility leading to an increase in the production of methane (Herrmann et al., 2021). Aqueous ammonia soaking improves lignin and xylan removal without inducing significant changes in the cellulose structure, enhancing hydrolysis (Yuan et al., 2020). The hydrothermal pretreatment is a heating process at a high temperature and pressure: hemicellulose and lignin are solubilized above 150 °C, while the solubilization of cellulose into sugars, aldehydes and other molecules initiates above 230 °C (Ahmed et al., 2019).

The present work evaluates the effect of two storage processes (solar drying, ensiling) and two thermal treatments (aqueous ammonia soaking, hydrothermal pretreatment) on the methane production potential of *Sparganium erectum*. Pretreatments were selected considering resources available in a full-scale biogas plant (water, energy and ammonia). This study aims to elucidate how these pretreatments affect methane production by analysing their effect on the plant's physicochemical characteristics, and and on the kinetics and microbial population involved in methane production.

2. Materials and methods

2.1. S. erectum biomass

The biomass, harvested from a lab-scale CWs, was the aboveground part of *S. erectum* because only this part is harvested in regular maintenance of industrial CWs. The lab-scale CWs treated liquid fraction of the digestate from a biogas plant (Porras-Socias et al., 2024). All *S. erectum* plants were collected once (November 2021) and stored at -20 °C in sealed plastic bags (5 kg/ bag). Unfrozen biomass was cut with scissors into 1 cm pieces approximately, simulating the size of industrial choppers. The fresh chopped biomass (FB) has a moisture content of 82.1 ± 0.3 %.

2.2. Pretreatments

FB were subjected to three different pretreatments that were selected considering their feasibility in a biogas plant: storage, since the biogas plant would have storage space; ammonia soaking, since ammonia aqueous solution would be recovered from the digestate; hydrothermal carbonization, since the biogas plant would have water and energy. The effectiveness of each pretreatment was evaluated with the biodegradation percentage, the potential methane yield and the net energy gain. Among, the morphological modification of the leaf tissues was qualitatively assessed (see E-supplementary materials).

Every pretreatment was done in triplicate.

The two storage conditions were dry and wet storage. The dry storage pretreatment (DS) was done by solar drying with 300 g of FB distributed homogenously in three aluminium trays (8.4 x 10.6 x 3.7 cm^3), following Prenafeta-Boldú et al. (2021). The drying process occurred for 14 days (December 2022) while monitoring the temperature, the air velocity inside the solar dryer and the weight of the trays. The maximal temperature was 45 ℃ and the final moisture of biomass was 8.94 %. Dried biomass was stored in sealed plastic bags at -20 °C.

The wet storage (WS) was conducted as a lab-scale ensiling. Vacuum bags were prepared with 100 g of FB at room temperature (25 °C) in dark conditions for 14 days, following Hillion et al., (2018). At day 14, the ensiled biomass was stored at -20 °C in sealed plastic bags.

The aqueous ammonia soaking pretreatments were conducted at two different temperature and time. For that, 100 g of FB were added to Pyrex bottles (2 L) with 610 mL of an aqueous ammonia solution (15 % w/w) (ammonia solution 32 %, Sigma-Aldrich, MO, USA). The liquid-solid ratio in each bottle was 1/1 (v/v), corresponding to 2.98 % of total solids (TS) of FB. Bottles were sealed to avoid NH_3 losses and left in darkness. One set of bottles was kept at room temperature (25 °C) for 96 hours (AAS) following Lymperatou et al., (2022), while another set was placed in an incubator at 51 °C for 27 hours (AAST) following Li et al., (2015). At the end of each pretreatment, the treated biomass was recovered first adding 610 mL of deionized water to each bottle, then performing a vacuum evaporation of the solution using a rotary evaporator (Rotavapor™ R-100, Büchi, Switzerland) at 130 mbar with an initial temperature of 20 °C that was progressively raised up till 80 °C, with a total duration of 80 min, following Lymperatou et al. (2017). After the vacuum evaporation, a liquid-solid separation of the substrate was performed by centrifugation at 13,000 g for 20 min at 4 °C (Eppendorf™ Centrifuge 5810 R, Germany). Both fractions (centrates AAS-L and AAST-L; and cakes AAS-S and AAST-S) were stored separately in sealed plastic bags at -20 °C.

For the hydrothermal pretreatment, 200 g of FB and 1,220 mL of deionized water were added in a high-temperature and high-pressure reactor (model Autoclave Zipperclave Pressure Vessel, Iberfluids S.A.,

Spain), keeping a liquid-solid ratio 1/1 (v/v). Two different conditions were performed: 2 hours at 120 °C (HT) following Vakalis et al., (2022); and 1 hour at 200 °C (HTC) following Ghimire et al., (2021). Reactions were under equilibrium pressure (< 2 bar at 120 °C and 14 bar at 200 °C for HT and HTC, respectively). When the reaction stopped, the product was cooled to room temperature (25 °C) and centrifuged at 13,000 g for 20 min at 4 °C. The centrate and the cake fractions (centrates HT-L and HTC-L; cakes HT-S and HTC-S) were stored separately in sealed plastic bags at -20 °C.

2.3. Chemical analysis

Samples were characterized with the content of total and volatile solids (TS, VS), pH, electrical conductivity (CE), total chemical oxygen demand (COD), total Kjeldahl nitrogen (TKN), total ammonium nitrogen (NH_4^+-N) (APHA et al., 2017). All analyses were performed in triplicates. The protein content was calculated with a conversion factor specific to vegetables following equation 1: protein = (TKN – NH_4^+) ·5.95 (Mariotti et al., 2008). The individual volatile fatty acids (VFA) content (acetate, propionate, iso-butyrate, n-butyrate, iso-valerate and n-valerate acids) was determined with a CP-3800 gas chromatograph (sample volume 0.3 μL; TRB-FFAP (30 m · 0.32 mm · 0.25 μm) capillary column at 90 °C; FID detector; Varian, Palo Alto, CA, USA). Only the cake fractions were analysed for fibres characterization, once lyophilized as powdered samples (CRYODOS-50 lyophilizer, Azbil Telstar, S.L.U., Terrassa, Spain). The hemicellulose and lignin content were determined by gravimetric analysis with a NaOH treatment and a two-stage acid hydrolysis, respectively; while the cellulose content was calculated based on the acid detergent fibre (ADF) and the acid detergent lignin (ADL) methods (AOAC international, 2019).

2.4. Biochemical methane potential test and kinetics

The six pretreated materials (DS, WS, AAS, AAST, HT and HTC-L) and the untreated FB were submitted to a biochemical methane potential (BMP) test in 1.2 L flasks (working volume 0.5 L), all prepared in triplicate. The AAS, AAST and HT samples were reconstructed maintaining the same percentage of centrate and cake phases, that were stored separately after centrifugation. Only the pH in the AAS and AAST bottles was neutralized (pH 7) with hydrochloric acid. In the case of HTC, only the centrate HTC-L was used for the BMP test, while the cake phase (hydrochar) was kept for other revalorization purposes.

The inoculum was collected in a mesophilic anaerobic digester treating sewage sludge (La Llagosta, Barcelona, Spain) and stored at 37 °C for two weeks to consume the residual organic matter. The substrate-to-inoculum ratio was adjusted to 1:1 based on VS content, except for the three control flasks (Ct) that contained no substrate, being the initial inoculum and substrate concentration of 5 g VS/L and 5 g COD/L, respectively. Bicarbonate (2.5 g/ vial) was added to buffer the medium, maintaining an optimum pH of 8.0 - 8.5. All bottles were sealed with rubber stoppers and flushed with N_2 for three minutes to ensure an anaerobic environment and then placed at 37 °C for 56 days. All vials were stirred manually once per day. The biogas production (CH_4, CO_2) was monitored three times a week with an Agilent CP-3800 gas chromatograph (sample volume 0,1 μL; Hayesep packed column Q 80/100 Mesh with 2 m × 1.8″ x 2.0 mm SS, at 90 °C; thermal conductivity detector; Varian, USA). At days 7, 13, 19, 26, 35, 41, 48 and 56, 1 mL of working volume per vial was collected and immediately centrifuged for 5 min at 20,000 g and 4 °C. The pellets were stored at - 80 °C for microbial community analysis and the supernatants were kept at – 20 °C to measure the VFA content. The total VFA and the net cumulative methane volume produced were expressed in terms of COD equivalents for comparison purposes. The biodegradability was assessed using the COD conversion efficiency, calculated as the ratio between the experimental methane yield (NmL CH4/g COD) ~~by~~ and the theoretical yield (350 NmL CH4/g COD). Pearson correlation coefficients were calculated to evaluate the relationship between these variables.

A non-linear least-square regression analysis was performed with the solver tool (Excel 2016) to fit the kinetics of the experimental methane production to the modified Stannard-Richards model (Zwietering et al., 1990), using the following equation 2: $BMP_t = A\ (1 + \upsilon \cdot \exp\ (1 + \upsilon) \cdot \exp\ ((\mu_m\ /A) \cdot (1 + \upsilon)\hat{}(1 + 1/\upsilon) \cdot (\lambda - t))\hat{}(-1/\upsilon)$, where BMP_t is the net methane production (NmL CH4 /g COD), being A is the maximum specific methane production potential (NmL CH4 /g COD), μ_m, is the maximum specific methane production rates (NmL CH4 /g COD · d), λ is the lag-phase time (d), t is the incubation time (d), and υ is the shape coefficient.

2.5. Molecular analysis

Both DNA and RNA were extracted simultaneously from pellet samples collected at days 7, 13, 19 (exponential growth phase) of the BMP test, with the RNeasy PowerMicrobiome kit following the manufacturer's instructions (Qiagen Inc., Venlo, Netherlands), while residual DNA (of RNA aliquot) was removed with RNase-free DNase I 2 U/μL (Applied Biological Materials Inc., Canada). Then, 20 μL of mRNA was reverse transcribed to cDNA with PrimeScript™ RT reagent Kit (Perfect Real Time; Takara Bio Inc., Kusatsu, Japan). cDNA concentration and purity were assessed through spectrophotometry (NanoDrop ND-2000 and Qubit 4 Fluorometer, Invitrogen, MA, USA). Archaea and bacteria functional profiles were assigned according to the FAPROTAX database (Louca et al., 2016). V4 region of 16S rRNA gene was amplified with the primer pair 515FB (GTGYCAGCMGCCGCGGTAA) and 806RB (GGACTACNVGGGTWTCTAAT), following the protocols from the Earth Microbiome Project. Amplicons were subjected to sequencing on an Illumina MiSeq sequencer with V3 chemistry (Illumina, San Diego, CA, USA) at Genoinseq (Cantanhede, Portugal). Data was processed following the method described in Porras-Socias et al. (2024). The sequencing data is available in the Sequence Read Archive of National Center for Biotechnology Information with accession number PRJNA1085251.

2.6. Data and statistical analysis

Each pretreatment was performed in triplicate. Each product was submitted to the BMP in triplicate. The averages and standard deviations were calculated with Microsoft Excel 2019 and statistical analysis were conducted with Sigmaplot software v 14.0. The Shapiro-Wilk test was used to first test the normality of the dataset with a confidence interval of 95 %. If the distribution was normal, an ANOVA test was performed, followed by a Tukey test to calculate the significant differences between the pretreatments with p values < 0.05. If not, a Kruskal-Wallis one-way ANOVA on ranks was used.

2.7. Energy balance assessment

The preliminary energy balance assessment was performed to estimate the feasibility of the integration of harvest biomass from CWs treatment as biogas feedstock, after being submitted to the described pretreatments. The assessment was performed based on the energy produced or consumed in kWh per 1 ton of substrate (untreated or pretreated) entering the reactor. For that, the equivalent tons of raw biomass were calculated. Four possible scenarios were considered depending on the hydraulic retention time (HRT) of the anaerobic mesophilic digester: 19, 25, 35, and 56 days. The assumed methane calorific value was 10.97 kWh/Nm^3; and the thermal and electric yield of a combined heat and power unit was 45 % and 36 %, respectively (Misson et al., 2020). The energy requirements were assumed as 16 kWh/ton for the chopper (Moiceanu et al., 2019) and 14.3 kWh/ton for the vacuum evaporator (Akbari Vakilabadi et al., 2019). The energy demand of the heating unit was calculate with the equation 3 (Lymperatou et al., 2022): Q= ρ ·V ·c ·(Tf – T0), being Q the heat demand (kJ), ρ the density of the substrate (kg/m^3), V the volume of the reactor

Table 1
Characteristics of the biomass before and after the pretreatments (n = 3). Notes: Underlined treatments denote that these materials were submitted to a BMP test. The symbol * indicates the reconstruction of sample with the corresponding cake (−S) and centrate (−L). The same letters indicate that there are no significant differences between groups with $p < 0.05$. Abbreviations: FB – chopped biomass, DS – dry storage, WS – wet storage, AAS – aqueous ammonia soaking at room temperature, AAST – aqueous ammonia soaking at 51 °C, HT – hydrothermally treatment at 120 °C, HTC – hydrothermal carbonization; nd: not determined; FW – fresh weight; VS – volatile solids; COD – chemical oxygen demand; EC – electrical conductivity; TKN – total Kjeldahl nitrogen; NH_4^+-N, total ammonia nitrogen.

Treatment	Moisture (% FW)	VS (% TS)	Ash (% TS)	COD (g O_2/ kg FW)	COD/VS ratio	pH	EC (mS/ cm)	TKN (g N/kg FW)	NH_4^+-N (% TKN)	methane yield ($NmLCH_4$/ gCOD)
FB	82.1 ± 0.3 a	86.3 ± 0.8 a	13.7 ± 0.8 a	254 ± 4 a	1.650 ± 0.007 ab	5.80 ± 0.02 a	nd	3.8 ± 0.3 a	12.2 ± 0.7 ab	103 ± 6
DS	9 ± 1b	86.0 ± 0.7 ab	14.1 ± 0.7 ab	1185 ± 79b	1.5 ± 0.1 ac	nd	nd	20 ± 2b	12.0 ± 1.0 a	121 ± 1
WS	83.6 ± 0.6c	84.1 ± 1.6 ab	15.9 ± 1.6 ab	219 ± 20 a	1.58 ± 0.09 ad	4.26 ± 0.07b	nd	3.3 ± 0.4 a	13.5 ± 0.9 ab	113 ± 10
AAS*	98.39 ± 0.09 d	78.6 ± 1.3c	21.4 ± 1.3c	20.4 ± 0.5c	1.36 ± 0.06 cd	11.4 ± 0.1c	4.6 ± 0.2 ab	14 ± 3c	76.0 ± 2.0c	140 ± 5
AAST*	98.44 ± 0.05 de	82 ± 1 bc	18 ± 1 bc	19.6 ± 0.4c	1.30 ± 0.02c	11.35 ± 0.09c	5.01 ± 0.02 a	13 ± 2c	92.0 ± 5.0 d	143 ± 13
HT*	97.5 ± 0.2 de	69 ± 3 d	31 ± 3 d	35 ± 3c	1.5 ± 0.2 ac	5.4 ± 0.1 d	4.24 ± 0.07b	0.51 ± 0.07 a	24.0 ± 4.0 e	122 ± 1
HTC-L	99.27 ± 0.03 e	69 ± 1 d	31 ± 1 d	9.2 ± 0.6c	1.84 ± 0.08b	3.77 ± 0.04 e	4.5 ± 0.3b	0.202 ± 0.001 a	22.0 ± 7.0 be	151 ± 3
HTC-S	92.1 ± 0.7	90 ± 2	10 ± 2	129 ± 2	1.8 ± 0.2	nd	nd	1.09 ± 0.15	9.0 ± 2.0	nd
AAS-L	99.60 ± 0.03	75 ± 2	25 ± 2	3.9 ± 0.2	1.33 ± 0.06	11.4 ± 0.1	4.6 ± 0.2	16 ± 3	76.0 ± 3.0	nd
AAS-S	94.3 ± 0.1	91.8 ± 0.5	8.2 ± 0.5	77 ± 7	1.5 ± 0.1	nd	nd	8 ± 3	73.0 ± 11.0	nd
AAST-L	99.43 ± 0.04	79 ± 1	21 ± 1	5.7 ± 0.2	1.26 ± 0.01	11.35 ± 0.09	5.01 ± 0.02	14 ± 2	94.0 ± 5.0	nd
AAST-S	94.0 ± 0.1	92.3 ± 0.9	7.7 ± 0.9	82 ± 2	1.49 ± 0.04	nd	nd	9 ± 1	79.0 ± 3.0	nd
HT-L	99.50 ± 0.04	55 ± 4	45 ± 4	4.1 ± 0.3	1.5 ± 0.3	5.4 ± 0.1	4.24 ± 0.07	0.12 ± 0.03	15.0 ± 18.0	nd
HT-S	94.2 ± 0.2	92 ± 1	8 ± 1	85 ± 4	1.58 ± 0.05	nd	nd	1.2 ± 0.2	26.0 ± 3.0	nd

(m^3), c the specific heat capacity of the substrate (kJ/kg·°C), T_f and T_0 the temperatures at the end and beginning of the heating process, respectively. The density and specific heat capacity of all materials were considered like water.

3. Results and discussion

3.1. Untreated and pretreated S. erectum characterization

FB physicochemical characterization is summarized in Table 1. The harvested biomass presented a TS content of 17.8 %, VS content of 86.3 %TS, comparable with the bur-reed literature values (Moeller et al., 2018), and an COD of 254 g/kg. The TKN and NH_4^+-N contents were 3.8 g N/kg and 12.2 %TKN respectively, also coherent with bur-reed TN values of Moeller et al., (2018). The COD/VS ratio of the untreated biomass was 1.65, reflecting a composition dominated by complex carbohydrates and recalcitrant lignin, typical of plant biomass. The cellulose, hemicellulose and lignin were 40 %, 24 % and 8 %VS, respectively (Table 2), like other macrophytes namely *Phragmites australis*, *Typha latifolia* or *Carex elata* (Czubaszek et al., 2021), and with lower lignin content, akin to *Egeria densa* (Dutra et al., 2024). The variability in the lignocellulosic content can be due to the plant species, the geographical location, the environmental conditions, and the maturity level (Czubaszek et al., 2021).

DS increased the TS content, reaching 91 %, with a slight decrease in VS, as observed in Papastefanakis et al. (2023), and a COD/VS ration of 1.5. However, WS slightly reduced TS and VS content to 16 % and 84 % TS (Table 1), respectively, also consistent with short-period ensiling studies (Herrmann et al., 2011), and a COD/VS ratio of 1.58. The ensiling process resulted in a pH drop to around 4, potentially indicating lactic acid fermentations (Sun et al., 2021). Both storage conditions had a minimal impact on the main components, showing a mild increase in hemicellulose and lignin and a decrease in cellulose.

The alkali and hydrothermal pretreatments significantly decreased both the TS and VS due to the addition of aqueous reagents and water. No dewatering steps of the biomass were included because each additional process would increase the pretreatments cost. The VS content in the centrate phase in AAS, AAST, HT, and HTC suggests the solubilization of organic matter from the plant tissues to the liquid phase, as previously observed (Kim et al., 2016; Poomsawat & Poomsawat, 2021). On the one hand, AAS and AAST treatments presented a significant reduction of COD/VS ratio, potentially indicating an increased proportion of readily digestible material. This effect is likely due to lignin solubilization, as supported by data in Table 2, where the lignin content decreased and the cellulose % rose, as previously observed (Yuan et al., 2020).

Ammonia has a high lignin selectivity, cleaving its linkages with carbohydrates and making them more accessible for microbial degradation (Kim et al., 2016). Regarding the hydrothermal pretreatments, the COD/VS ratio was 1.54 for HT and 1.81 for HTC-L, with the increased value in HTC-L, suggesting a relative reduction of the carbohydrates fraction and potential solubilization of non-digestible lignin products. The pH of HTC-L was 3.8, consistent with the production of organic acids during biomass hydrolysis (Poomsawat & Poomsawat, 2021). In the cake fraction, cellulose and lignin were relatively concentrated, and hemicellulose was significantly reduced (Table 2). This indicates that hemicellulose was preferentially solubilized and mobilized to HTC-L, which likely contained readily available substrates such as sugars, organic acids, and oligomers from hemicellulose, and smaller amounts of solubilized lignin and cellulose fragments (Nguyen et al., 2023). In addition, the cellulose and lignin content of HT-S was also relatively concentrated, as reported previously (Dutra et al., 2024).

Therefore, apparently, the pretreatment offering the best improvement of anaerobic digestibility of *S. erectum*, would be AAST due to its high cellulose content, and lower hemicellulose and lignin content, diminishing the complexity of the leaf structure, facilitating enzymatic hydrolysis (Lymperatou et al., 2017). Furthermore, it was noted that for both alkali and hydrothermal pretreatments, higher temperature resulted in greater effect on organic matter solubilization, which was reflected in higher COD and VS content in the centrate (Li et al., 2015; Yuan et al., 2020; Vakalis et al., 2022).

Table 2
Content of cellulose, hemicellulose and lignin content of S. erectum (n = 3) after the pretreatment (FB) and before the pretreatment (DS, WS, AAS-S, AAST-S and HT-S). The same letters indicate that there are no significant differences between groups with $p < 0.05$. Abbreviations: nd: not determined; TS – total solids; VS – volatile solids; DS – dry stored biomass, WS – wet stored biomass, AAS-S – cake fraction after aqueous ammonia soaking pretreated biomass at room temperature, AAST-S – cake fraction after aqueous ammonia soaking at 51 °C, HT-S – cake fraction after hydrothermal treatment at 120 °C, HTC-S – cake fraction after hydrothermal carbonization.

Treatment	Before anaerobic digestion				After anaerobic digestion				
	Cellulose (% VS)	Hemicellulose (% VS)	Lignin (% VS)	Degradation efficiency (%)	Cellulose (% VS)	Hemicellulose (% VS)	Lignin (% VS)	TS (%)	VS (%)
FB	40 ± 4 ab	24 ± 2 ab	8 ± 1 a	74 ± 8	18.4	8.6	14.1	90.2	57.5
DS	39 ± 2 ab	27 ± 2 a	8 ± 1 a	85 ± 2	16.8	11.3	16.7	89.5	61.0
WS	36 ± 5 a	27 ± 2 a	8 ± 2 a	80 ± 3	18.4	11.1	16.6	91.4	61.6
AAS-S	43 ± 2 abc	21.5 ± 0.9 ab	6.2 ± 0.4 a	94 ± 1	6.0	1.9	12.0	91.8	62.6
AAST-S	45 ± 2 bc	14 ± 3c	6 ± 1 a	107 ± 1	5.5	1.0	9.1	92.0	61.1
HT-S	45 ± 2 bc	20 ± 4b	11.9 ± 0.2b	86 ± 2	16.1	5.1	15.1	92.9	59.4
HTC-S	49.5 ± 0.9c	3.3 ± 0.9 d	18 ± 1c	nd	nd	nd	nd	nd	nd

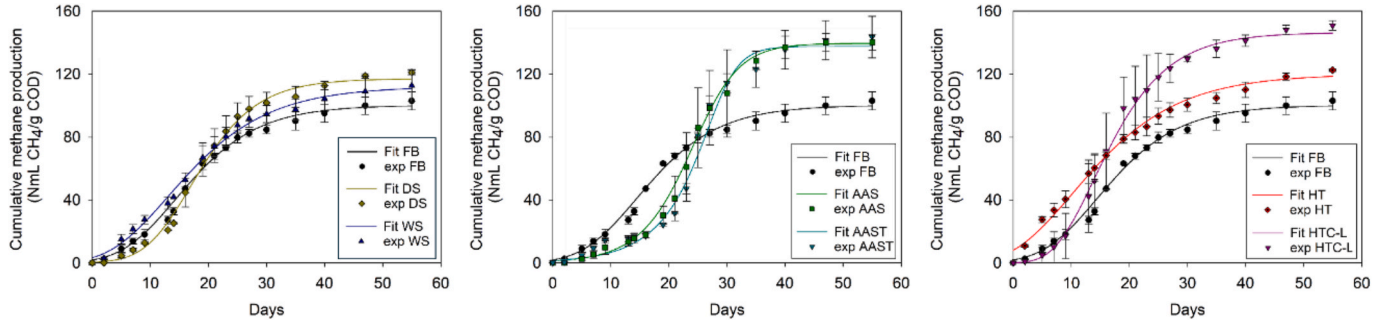


Fig. 1. Net cumulative methane yield of BMP experiments of untreated and pretreated biomass (n = 3). Dots represent the experimental data, while the lines correspond to the fit to the Stannard-Richards model for each batch. Abbreviations: FB – untreated biomass, DS – dry storage, WS – wet storage, AAS – aqueous ammonia soaking at room temperature, AAST – aqueous ammonia soaking at 51 °C, HT – hydrothermally treatment at 120 °C, HTC-L – centrate phase after hydrothermal carbonization.

The TKN content of DS rose significantly (Table 1), due to a concentration effect because of the loss of water content, while its NH_4^+-N percentage did not vary from FB. During ensiling, NH_4^+-N percentage increased mildly, thus, apparently, no protein degradation occurred (Sun et al., 2021). However, aqueous ammonia treatments increased significantly the TKN and NH_4^+-N of pretreated biomass, due to the addition of NH_4OH solution. Finally, hydrothermal pretreatments decreased the TKN content, due to the addition of water, and increased significantly the NH_4^+-N in % TKN, elucidating the potential breakdown of cell structures, proteins or other organic compounds releasing NH_4^+ (Ahmed et al., 2019).

The pretreatments changed the surface structure of the biomass, probably improving the accessibility of the lytic enzymes. The untreated biomass presented compacted epidermal cells and a smooth surface (figure S2; E-supplementary). DS and WS shared a similar morphology, featuring flattened cells with low relief and showing some pores in WS. In contrast, aqueous ammonia soaking induced significant morphological changes, with AAS exhibiting numerous pores (<50 μm) in the cell wall, and AAST presenting larger pores (about 150 μm) and apparent fibre detachment. HT showed fissures (about 100 μm wide and over 600 μm long) on the leaf epidermis, despite the remaining parts of the surface preserved integrity, while HTC resulted in a high degree of disruption. These morphological changes are consistent with previous studies on similar pretreatments of *E. densa* (Dutra et al., 2024) and rice straw (Yuan et al., 2020). Therefore, apparently, the pretreatment causing more damage to the epidermal morphology, allowing the anaerobes to increase the digestibility of the biomass were HTC, AAST and HT.

3.2. *Effect of the pretreatment on the methane yield*

Fig. 1 shows the cumulative methane yield curves. A 3-day lag phase was shown for FB (table S1; E-supplementary), followed by an exponential phase culminating in a methane yield of 80 NmL CH_4/g COD at day 25, and finally a gradual increase resulting in a final yield of 103 NmL CH_4/g COD at day 56, which is comparable with untreated seaweed (Lymperatou et al., 2022).

DS and WS showed similar profiles with slightly higher yields, reaching 121 and 113 NmL CH_4/g COD on average, respectively, having the least effect on methane yield among all pretreatments. Dried biomass appeared to hinder bacterial growth due to reduced moisture and nutrient accessibility (Moussaoui et al., 2024). Similarly, ensiling serves mainly as a storage method, with limited improvements in methane yield (Herrmann et al., 2011), and with increases mainly seen after extended silage periods due to increasing ethanol concentration (Sun et al., 2021).

Alkali pretreatments (AAS and AAST) resulted in a longer lag phase of 16 days (table S1; E-supplementary), likely due to initial inhibition of microbial activity by high ammonia concentrations or dissolved lignin produced during the alkali pretreatment (Yang et al., 2018). Subsequently, the methane yield exhibited an exponential growth, surpassing the methane yield of FB at day 25, reaching 140 NmL CH_4/g COD for AAS and 143 NmL CH_4/g COD for AAST at the end of the experiment with no significant differences between them. While these values represent a 28 and 31 % increase, respectively, this is lower than previously found for other substrates (Lymperatou et al., 2022).

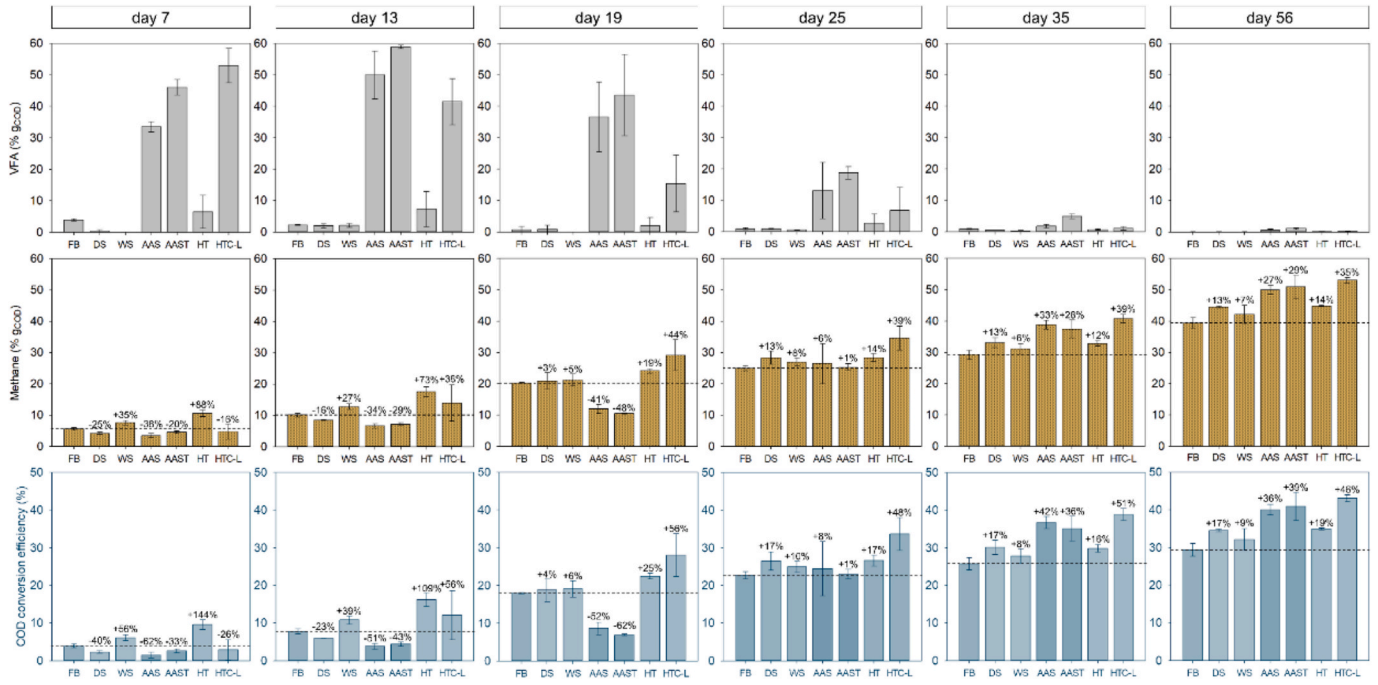


Fig. 2. Conversion efficiency of the initial organic matter, expressed as chemical oxygen demand (COD), into volatile fatty acids (VFA) or methane after 7, 13, 19, 25, 35 and 55 days of the biochemical methane potential test (n = 3). The dashed black lines indicate the FB level and the percentages on the top of the bars present the increase of methane or COD conversion efficiency compared to FB. Abbreviations: FB – fresh untreated biomass, DS – dry storage, WS – wet storage, AAS – aqueous ammonia soaking at room temperature, AAST – aqueous ammonia soaking at 51 °C, HT – hydrothermal treatment at 120 °C, HTC-L – centrate fraction after hydrothermal carbonization.

HT presented the highest cumulative methane yield during the first 16 days but then was surpassed by HTC-L. HT yield gradually rose throughout the experiment reaching a final yield of 122 NmL CH_4/g COD. It represents a 12 % increase in methane yield, falling within the range reported in previous studies (Luo et al., 2019). HTC-L had a short lag phase of 7 days (table S1; E-supplementary), reaching a final yield of 151 NmL CH_4/g COD, a 38 % increase in methane yield. This increase is supported by previous studies since hydrothermal carbonization facilitates cell disruption, releasing available organic compounds (Nguyen et al., 2023).

The Stannard-Richards kinetic model successfully simulated the experimental results (Fig. 1), with R^2 values higher than 99.05 % (table S1; E-supplementary). The parameters A and λ values fitted well with experimental results. Notably, the model revealed that HT had no lag phase, while AAS and AAST showed the longest lag phases, 15 and 18 days, respectively, which correlates with experimental data. Moreover, the kinetic model predicted that the most suitable pretreatment given its high methane yield and relatively short lag phase, was hydrothermal carbonization, as HTC-L produced 146 NmL CH_4/g COD with a lag phase of 7 days.

Fig. 2 illustrates the VFA and methane yields and the global COD conversion efficiency, all expressed as percentage of the initial COD. VFA yield presented a positive correlation with COD conversion efficiency on day 19 (r = 0.7313), indicating that higher VFA levels were associated with COD degradation in the early AD phase. From day 25 onwards, the methane yield showed a strong positive correlation with COD conversion efficiency (r>0.999). FB showed the highest VFA production on day 7 (3.9 %), while DS and WS treatments presented low VFA levels.

In the initial 5 days, easy-biodegradable compounds are the hydrolysed (Dutra et al., 2024). The lack of a VFA peak confirmed the absence of an exponential phase of methane yield in FB, DS and WS, although the 2 % as VFAs on day 13 led to the steepest methane increase, suggesting a coordinated acetogenic-methanogenic activity. A progressive but low COD conversion into methane (29 - 35 % at day 56) reflected *S. erectum* recalcitrance, that could not be overcome by the storage's methods.

The HT also presented low VFA levels but a higher initial COD conversion into methane, over 73 % as compared to FB, which then stabilized around 12 – 19 % after day 19. The pretreatment potentially accelerated hydrolysis and acidogenesis reaching the highest VFA levels in the initial period (Luo et al., 2019), and increased the lignocellulosic substrate's carbohydrates availability (Dutra et al., 2024) but had limited effect in the long term likely due to the recalcitrance of the biomass. However, this pretreatment may be suitable for AD processes with short retention times.

In contrast, AAS, AAST and HTC-L had higher VFA production, peaking between days 7 and 19, and alkali-pretreated biomass presented an initial inhibition in methane conversion with low COD conversion efficiencies. It was only from day 35 onward that this value exceeded FB levels by more than 36 %. High VFA levels can indicate inhibition of acetogenesis and methanogenesis due to ammonia or other factors (Luo et al., 2019; Yang et al., 2018). Overall, at the end of the experiment, the highest methane yields were achieved by HTC-L, AAST and AAS, confirming that these three pretreatments increased the biodegradability of *S. erectum* biomass, especially hydrothermal carbonization. The degradation efficiency followed this trend, being AAS and AAST the pretreatments enhancing the degradation efficiency (94 and 107 %), potentially due to the disruption of the lignin enhancing carbohydrate accessibility (Lymperatou et al., 2022), and DS, WS and HT the ones with less pronounced biodegradability improvements (80 – 86 %; Table 2).

After the BMP test, the surface structure of all biomasses, raw and pretreated, were damaged (figure S1; E-supplementary). Despite the degradation of the leaf's tissues, FB, DS and WS products maintained epidermal or mesophyll cells and vascular tissues. However, in AAS and AAST, the initial morphology of the leaf surface was unrecognizable, forming a spherical conglomerate with fibres that hadn't been degraded. As for HT products, micrographs show the opening of the leaf, exposing

the internal cavities undergoing degradation. Overall, the aqueous ammonia soaking pretreatments presented at the end of AD process more apparent biomass degradation.

3.3. Effect of the pretreatments on the microbial communities

Fig. 3 illustrates the taxonomic profiles of the reactors' microbiota at the phylum and genus levels. Metabolically active prokaryotes in AD were analysed at three days (7, 13 and 19) during the exponential phase of methane production. Both AAS and AAST presented the lowest prokaryotic richness and Shannon diversity index, indicating a decrease of the diversity of the community with significant differences with the other treatments (table S2 and figure S2; E-supplementary data). The aqueous ammonia treatments exerted a selective pressure on the microbiome. In terms of beta diversity, only FB and stored biomass presented no significant differences (PERMANOVA, $p = 0.077$), while significant differences were observed ($p < 0.001$) between all the other treatments (table S2 and figure S2; E-supplementary data), indicating that aqueous ammonia and hydrothermal pretreatments led to shifts in the reactors' prokaryotic population.

In general, FB, DS and WS presented similar profiles, with *Acetothermia, Cloacimonadota* and *Halobacterota*, being the most abundant phyla at day 7, and *Desulfobacterota* gaining dominance at day 19. In addition, HT showed minimal variation in the taxonomic profile over time, where *Cloacimonadota, Actinobacteriota, Firmicutes* and *Acetothermia* were the predominant communities. The ~~reactors'~~ inoculum seemed to drive the microbial profiles rather than the pretreatment conditions of the feedstock, as similar taxonomic patterns appeared across FB, DS, WS, and HT reactors as compared with Ct.

The analyses of the functional metabolic pathways of these treatments confirmed that, while several pathways were found, fermentation and chemoheterotrophs were the most prominent (figure S3; E-supplementary data), both playing a critical role in hydrolysis and acidogenesis stages of AD (Harirchi et al., 2022). In addition, sulphate respiration metabolism was also statistically significant, indicating that sulphate reducing bacteria could outcompete with acetogens and methanogens (Harirchi et al., 2022).

However, HTC-L, AAS and AAST presented clear population shifts from Ct. HTC-L reactors were dominated by *Actinobacteriota* (Fig. 3), potentially related to the substrate's low pH and putatively high sugar and organic acids availability (Nguyen et al., 2023), or their ability to degrade lignocellulosic compounds (Perman et al., 2022), their syntrophic interactions with acetogens and methanogens facilitating the production of VFAs, and for their adaptability to low pH conditions (Liu et al., 2023). The functional analysis (figure S3; E-supplementary data) confirmed this shift, showing that HTC-L significantly enhanced fermentation, chemoheterotrophy, and nitrogen compounds respiration, which may be due to the solubilization of nitrogen from protein breakdown and other organic compounds (Nguyen et al., 2023). In contrast, AAS and AAST reactors were dominated by *Firmicutes, Bacteroidota,* and *Spirochaetota*, presenting a notorious shift from Ct, also found in reactors with high levels of ammonia (Yang et al., 2018). These phyla are often associated with syntrophic acetate-oxidizing bacteria that metabolize acetate excess due to the ammonia inhibition of acetotrophic methanogens (Ruiz-Sánchez et al., 2018).

At the genus level, the treatments harboured numerous fermentative bacteria involved in hydrolysis, acidogenesis, and acetogenesis. Generally, FB, DS, WS, HT and HTC-L displayed taxonomic profiles like Ct. *Cloacimonadaceae* W5, unclassified W27 and *Candidatus Caldatribacterium* had abundances over 5 % on day 7, and *Syntrophorhabdus* increased at day 19. These genera have been previously reported in AD reactors and are propionate oxidizers, with degradation capacity of cellulosic metabolites and phenolic compounds in association with hydrogenotrophic methanogens (Perman et al., 2022; Usman et al., 2023; Struckmann Poulsen et al., 2022). The presence of *Clostridium* sensu stricto 1 in FB, DS, and WS, suggest that this organism with cellulolytic activity also could contribute to the stability of the system (Struckmann Poulsen et al., 2022).

Regarding hydrothermal pretreatments, the prokaryotic community of the reactor showed stability over time. HT and HTC-L reactors were similarly dominated by Cloacimonadaceae W5, unclassified W27, *Candidatus* Caldatribacterium and unclassified Spirochaetaceae, and HTC-L reactors also presented higher abundances of Microtrichaceae that is related to the degradation of organic nitrogen in nitrification-anammox systems and the hydrolysis of complex organic matter (Guo et al., 2022).

However, the taxonomic profile of AAS and AAST reactors differed from the Ct. On day 7, the most abundant genera were *Treponema*, known for its capacity to hydrolyse lignocellulosic biomass and its positive cellulase activity correlation, and *Hungateiclostridium UCG-012*, which is related to carbohydrate hydrolysis and fermentation with a potential for methane production inhibition. Both genera are described as assimilating ammonia (Cazaudelhore et al., 2022; Jensen et al., 2021). *Ruminofilibacter*, a genus with xylan and hemicellulolytic activities, was also prevalent (Wang et al., 2020). This could indicate a dominance of hydrolytic and acidogenic activity in the initial stages of the digestion, supported by the analysis of metabolic pathways (figure S3; E-supplementary data). At days 13 and 19, less abundant taxa such as, *Longilinea* which can ferment sugars to produce acetate, lactate, and H_2, and *Thermovirga*, that can oxidize acetate, gained prevalence suggesting a shift from primary hydrolysers to organisms involved in intermediate metabolism (Wang et al., 2023).

The activity of other detected genera such as *Romboutsia*, active in acidogenesis by fermenting carbohydrates and amino acids to formate and acetate, *Syner-01*, *Syntrophorhabdus* and *Syntrophobacter,* that are syntrophic VFA-oxidizing bacteria producing H_2, acetate and other VFAs, and *Acetobacterium*, that consumes H_2 and CO_2 to form acetate, highlights the complex interactions within the AD (Jensen et al., 2021; Harirchi et al., 2022).

The methanogenic archaeal community belonging to the *Halobacterota* phylum, exhibited relatively high abundance in FB, DS and WS reactors. *Methanoculleus* and *Methanosaeta* were the dominant genera, while *Methanobacterium* and *Methanomethylovorans* were less prevalent. *Methanosaeta*, an acetoclastic methanogen, is typically associated with stable conditions and low ammonia concentrations, whereas *Methanoculleus* are hydrogenotrophic methanogens tolerant to high ammonia concentrations (Harirchi et al., 2022). In FB, DS and WS both *Methanoculleus* and *Methanosaeta* presented relative abundances between 6.4 and 9.5 % on day 7. In contrast, in AAS, AAST and HTC-L, only *Methanoculleus* emerged as one of the most dominant genera, with 11.7, 4.6 and 5.9 %, respectively, with *Methanosaeta* having minimal presence, likely due to the higher ammonia and/or acetate levels that inhibited the obligate acetotrophic genus (Ruiz-Sánchez et al., 2018).

Overall, the methanogenic community structure appeared more influenced by the ammonia concentrations than by substrate type. The active microbial community potentially showed strong syntrophic cooperation, balancing VFA production and consumption for methanogenesis. However, only few detected genera were directly related to complex-carbon hydrolysers, suggesting a limited capacity for lignocellulosic biomass processing (Basak et al., 2025).

3.4. Energy balance of S. erectum pretreatments

The preliminary energy balance of the different pretreatments was assessed by comparing the net energy obtained from methane production (heat and electricity) with the energy consumed during pretreatments. Table 3 presents the analysis for different scenarios based on the HRT of the digester (19, 25, 35, 56 days). DS yielded the highest net energy gain (630 kWh on day 19; 1,234 kWh on day 56) with a 474 % increase over FB energy production.

The energy requirements of aqueous ammonia soaking and hydrothermal pretreatments were high, leading to processes not

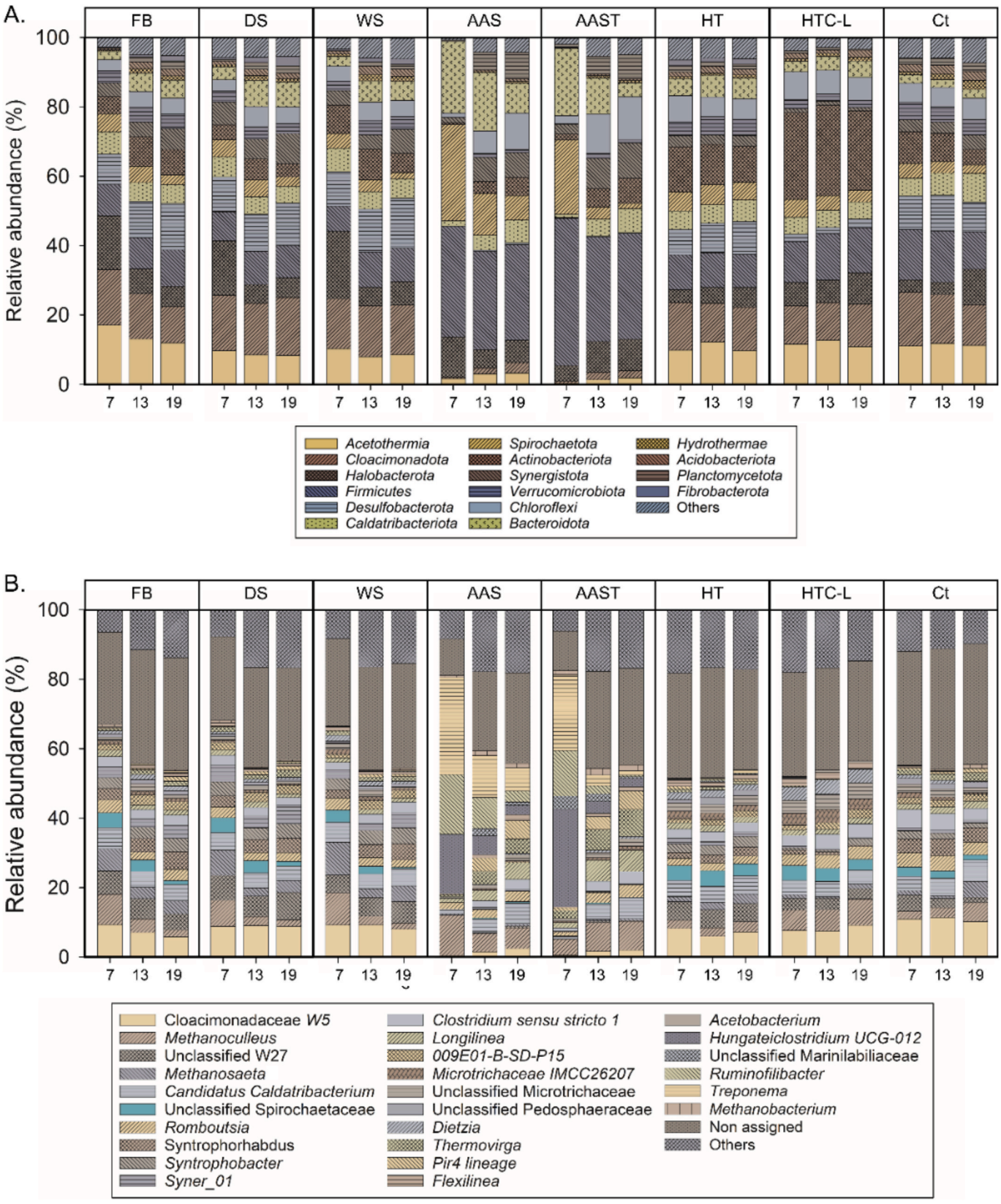


Fig. 3. Taxonomic profile of most metabolically active prokaryotic communities in the reactors at day 7, 13, and 19. Average (n = 3) relative abundance for each substrate conditions (untreated – FB; pretreated – DS, WS, AAS, AAST, HT, and HTC-L; and inoculum without substrate –Ct) are presented at phylum level (A) and genus level (B). Others correspond to phyla and genera with abundances below 2 %. Abbreviations: FB – fresh untreated biomass, DS – dry storage, WS – wet storage, AAS – aqueous ammonia soaking at room temperature, AAST – aqueous ammonia soaking at 51 °C, HT – hydrothermally pretreated biomass at 120 °C, HTC-L – centrate phase after hydrothermal carbonization at 200 °C, Ct – control without substrate.

Table 3
Preliminary energy balance assessment of pretreatments of *S. erectum* biomass combined with anaerobic digestion, including the net energy gain compared to the energy produced by chopped biomass (FB). The study considered the energy consumption to pretreat 1 ton of substrate entering the digesters and the energy produced based on experimental methane yields. Abbreviations: AD – anaerobic digestion; HRT- hydraulic retention time; FB – chopped untreated biomass, DS – dry storage, WS – wet storage, AAS – aqueous ammonia soaking at room temperature, AAST – aqueous ammonia soaking at 51 °C, HT – hydrothermal treatment at 120 °C, HTC-L – centrate fraction after hydrothermal carbonization.

Treatment	Energy demand (kWh)	AD-HRT 19 days			AD-HRT 25 days			AD-HRT 35 days			AD-HRT 56 days		
		production (kWh)	Energy balance (kWh)	Net gain (% energy FB)	production (kWh)	Energy balance (kWh)	Net gain (% energy FB)	production (kWh)	Energy balance (kWh)	Net gain (% energy FB)	production (kWh)	Energy balance (kWh)	Net gain (% energy FB)
FB	16	141	125	0 %	178	162	0 %	202	186	0 %	231	215	0 %
DS	9	718	630	404 %	1017	928	473 %	1154	1065	473 %	1323	1234	474 %
WS	16	130	114	−9 %	170	154	−5 %	189	174	−6 %	219	203	−6 %
AAS	28	5	−23	−118 %	16	−13	−108 %	23	−5	−103 %	25	−3	−101 %
AAST	63	4	−58	−146 %	14	−49	−130 %	21	−41	−122 %	25	−38	−118 %
HT	118	25	−93	−174 %	30	−89	−155 %	34	−85	−146 %	39	−79	−137 %
HTC-L	260	7	−252	−302 %	9	−251	−255 %	11	−249	−234 %	12	−248	−215 %

energetically viable. This contrast with previous studies which presented positive outcomes with those pretreatments (Lymperatou et al., 2022).

The improvement in methane yield observed with DS was minor, which indicates that the effect of DS was limited in the predigestion of *S. erectum*. However, it is a suitable pretreatment to store biomass before digestion, and to produce dried biomass that could be used a co-substrate with highly biodegradable or N-rich substrates, as it enhances methane yield (Papastefanakis et al., 2023).

The use of ensiling and solar drying, with their low impact in biomass composition, did not overcome the recalcitrance of *S. erectum* leaves, and the results suggest they act as a storage method by preserving the biomass, and enhance slightly the methane yield. In contrast, although both ammonia and hydrothermal pretreatments had a negative energy balance, they enhanced the biogas production by improving the biodegradability of the biomass.

The presented study only provides a preliminary feasibility assessment of different pretreatments to be applied in biogas plants working with bur-reeds. Further attention should be directed towards the optimization of these pretreatments, tailored to the specific macrophyte specie, to release cellulose and hemicellulose from lignin and unlock its potential methane yield, considering the significant impact of pretreatments on the overall process cost. Therefore, future assessments about aqueous ammonia soaking and hydrothermal pretreatments should focus on optimizing the liquid-solid ration in the reactors or exploring the digestion of only the cake fractions, even if it would involve a centrifugation step into the industrial process.

Several studies show that biogas yield is affected by C:N ratio while the biomass from wetlands often falls outside the optimal range of 20-30 for the growth of methanogens (Czubaszek et al., 2021). Therefore, co-digestion potential of *S. erectum* with other substrates such as animal manure might be optimized to adjust the C:N ratio, as co-digestion particularly improves hydrolysis and methanogenesis (Kaushal et al., 2022). In addition, it is important to consider the harvest~~ing~~ period because the methane yield differs significantly depending on the mowing season. The biomass in this work was harvested in Novembre, while higher energy yields have been reported for macrophytes with a cutting period between July and August (Czubaszek et al., 2021).

4. Conclusion

This study evaluated the effect of storage, aqueous ammonia soaking and hydrothermal pretreatments to enhance the methane yield of *S. erectum* harvested from constructed wetlands. This study explores energy recovery options from aquatic weeds, promoting circular economy principles. Storage resulted in mild alterations in biomass composition and structure, while alkali and hydrothermal pretreatments led to notable effects. All pretreated biomass improved the methane yield, but hydrothermal carbonization presented the highest increase, reaching 46 %. At a microbiological level, the inoculum mainly drove the taxonomic profiles of reactors, with numerous active fermentative and syntrophic bacteria genera. However, alkali pretreatment led to a significant shift in the population and a taxa abundance decrease. These findings underscore the importance of pretreatments for AD of macrophytes, being dry storage is more feasible, because it is more economical and support the need of further optimization of aqueous ammonia soaking and hydrothermal carbonization to achieve a feasible outcome.

CRediT authorship contribution statement

Pau Porras-Socias: Writing – original draft, Visualization, Validation, Methodology, Investigation, Formal analysis, Data curation, Conceptualization. **Miriam Guivernau:** Writing – review & editing, Writing – original draft, Resources, Methodology. **Alexandre B. De Menezes:** Writing – original draft, Supervision. **Carlos R. Gomes:** Writing – original draft, Supervision. **C.Marisa R. Almeida:** Writing –

original draft, Supervision. **Ana Paula Mucha:** Writing – original draft, Supervision. **Belén Fernández:** Writing – review & editing, Writing – original draft, Validation, Supervision, Resources, Methodology, Data curation, Conceptualization.

Declaration of competing interest

The authors declare that they have no known competing financial interests or personal relationships that could have appeared to influence the work reported in this paper.

Acknowledgements

The authors declare that financial support was received for the research, authorship, and/or publication of this article. This project has received funding from the European Union's Horizon 2020 Research and Innovation Programme under the Marie Skłodowska Curie Grant Agreement no. 861088. The authors would like to thank Neus Bonet-Garcia, Veronica Baldasso, and Guna Bavithra from CIIMAR for their valuable assistance harvesting the biomass, Marlene Mendoza from IRTA for her constant assistance in all stages of the research, Yolanda Lucas and Mar Carreras-Sempere from IRTA for their help during the microbiological analysis, VFA sampling and bioinformatic analysis, Laura Tey from IRTA for enhancing interesting discussions, and Claudia Cardazo, Laura Garcia, Anna Puerta, and Eva Romero from IRTA for their help with physicochemical analysis. CIIMAR Strategic Funding UIDB/04423/2020 and UIDP/04423/2020 through national funds provided by FCT and the European Regional Development Fund (ERDF) is also acknowledged. IRTA thanks for the funds provided by the Spanish Agencia Estatal de Investigación (PID2020-119312RR-I00, BIOUPRISE project), and the Consolidated Research Group SOSBIO (ref. 2021 SGR 01568 Generalitat de Catalunya) and the support of the CERCA Programme from the Generalitat de Catalunya.

Appendix A. Supplementary data

Supplementary data to this article can be found online at https://doi.org/10.1016/j.biortech.2026.135822.

Data availability

Data will be made available on request.

References

Abraham, A., Mathew, A.K., Park, H., Choi, O., Sindhu, R., Parameswaran, B., Pandey, A., Park, J.H., Sang, B.I., 2020. Pretreatment strategies for enhanced biogas production from lignocellulosic biomass. Bioresour. Technol. 301. https://doi.org/10.1016/j.biortech.2019.122725.

Ahmed, B., Aboudi, K., Tyagi, V.K., álvarez-Gallego, C. J., Fernández-Güelfo, L. A., Romero-García, L. I., & Kazmi, A. A, 2019. Improvement of anaerobic digestion of lignocellulosic biomass by hydrothermal pretreatment. Applied Sciences (Switzerland) 9, 3853. https://doi.org/10.3390/app9183853.

Akbari Vakilabadi, M., Bidi, M., Najafi, A.F., Ahmadi, M.H., 2019. Energy, Exergy analysis and performance evaluation of a vacuum evaporator for solar thermal power plant Zero Liquid Discharge Systems. J. Therm. Anal. Calorim. 139, 1275–1290. https://doi.org/10.1007/s10973-019-08463-7.

Alam, S.N., Khalid, Z., Guldhe, A., Singh, B., Korstad, J., 2021. Harvesting and pretreatment techniques of aquatic macrophytes and macroalgae for production of biofuels. Environmental Sustainability 4 (2), 299–316. https://doi.org/10.1007/s42398-021-00178-6.

AOAC international. (2019). Official Methods of Analysis (G. W. Latimer, Ed.; 21st ed.).

APHA, AWWA, & WEF. (2017). Standard Methods for the Examination of Water and Wastewater (R. Baird, A. D. Eaton, E. W. Rice, & L. Bridgewater, Eds.; 23rd ed.).

Basak, B., Kumar, R., Tanpure, R.S., Mishra, A., Tripathy, S.K., Chakrabortty, S., Jeon, B. H., 2025. Roles of engineered lignocellulolytic microbiota in bioaugmenting lignocellulose biomethanation. Renew. Sustain. Energy Rev. 207, 114913. https://doi.org/10.1016/j.rser.2024.114913.

Cinar, S.Ö., Wieczorel, N., Kosheleva, A., Küçüker, M.A., Kuchta, K., 2022. Biogas production from aquatic biomass. In: Pandey, V.C. (Ed.), Algae and Aquatic Macrophytes in Cities, (1st ed.,. Elsevier, pp. 203–231.

Czubaszek, R., Wysocka-Czubaszek, A., Wichtmann, W., Banaszuk, P., 2021. Specific methane yield of wetland biomass in dry and wet fermentation technologies. Energies 14, 8373. https://doi.org/10.3390/en14248373.

Dotro, G., Langergraber, G., Molle, P., Nivala, J., Puigagut, J., Stein, O., & Von Sperling, M. (2017). Overview of treatment wetlands. In Treatment Wetlands (1st ed., Vol. 7, pp. 18–21). IWA Publishing. doi: 10.2166/9781780408774.

da Dutra, J., C. F., Passos, M. F., Moretti, É. R., do Nascimento, L. A. S., da Silva, A. J., da Silva, T. F., Aguiar, R. H., dos Santos Rodrigues, L., & Mockaitis, G, 2024. Methane production from lignocellulosic biomass using hydrothermal pretreatment. Biomass Convers. Biorefin. 14, 3699–3713. https://doi.org/10.1007/s13399-022-02604-z.

Fletcher, J., Willby, N., Oliver, D.M., Quilliam, R.S., 2020. Phytoremediation using aquatic plants. In: Shmaefsky, B. (Ed.), Phytoremediation. Concepts and Strategies in Plant Sciences. Springer, Cham, pp. 205–260. https://doi.org/10.1007/978-3-030-00099-8_7.

Ghimire, S., Wang, L., Zhang, B., Li, X., Shahbazi, A., 2021. Production and modification of hydrochar from anaerobically digested cattail for adsorbing ammonium and phosphorous in wastewater. Water Sci. Technol. 84 (7), 1678–1692. https://doi.org/10.2166/wst.2021.378.

Gottsberger, G., 2020. Sparganium erectum (Typhaceae) and its ambophilous characteristics. Phyton 60, 21–25. https://doi.org/10.12905/0380.phyton60-2020-0021.

Guo, R., Ma, X., Zhang, J., Liu, C., Thu, C.A., Win, T.N., Aung, N.L., Win, H.S., Naing, S., Li, H., Zhou, F., Wang, P., 2022. Microbial community structures and important taxa across oxygen gradients in the Andaman Sea and eastern Bay of Bengal epipelagic waters. Front. Microbiol. 13, 1041521. https://doi.org/10.3389/fmicb.2022.1041521.

Harirchi, S., Wainaina, S., Sar, T., Nojoumi, S.A., Parchami, M., Parchami, M., Varjani, S., Khanal, S.K., Wong, J., Awasthi, M.K., Taherzadeh, M.J., 2022. Microbiological insights into anaerobic digestion for biogas, hydrogen or volatile fatty acids (VFAs): a review. Bioengineered 13 (3), 6521–6557. https://doi.org/10.1080/21655979.2022.2035986.

Herrmann, C., Heiermann, M., Idler, C., 2011. Effects of ensiling, silage additives and storage period on methane formation of biogas crops. Bioresour. Technol. 102 (8), 5153–5161. https://doi.org/10.1016/j.biortech.2011.01.012.

Hillion, M.L., Moscoviz, R., Trably, E., Leblanc, Y., Bernet, N., Torrijos, M., Escudié, R., 2018. Co-ensiling as a new technique for long-term storage of agro-industrial waste with low sugar content prior to anaerobic digestion. Waste Manag. 71, 147–155. https://doi.org/10.1016/j.wasman.2017.10.024.

Hu, F., Zhang, S., Wang, X., Wang, C., Wu, J., Xu, L., Xu, G., Hu, Y., 2022. Investigating the role of different materials supplementation in anaerobic digestion of kitchen waste: Performance and microbial community dynamics. Biochem. Eng. J. 184, 108490. https://doi.org/10.1016/j.bej.2022.108490.

Jensen, M.B., de Jonge, N., Dolriis, M.D., Kragelund, C., Fischer, C.H., Eskesen, M.R., Noer, K., Møller, H.B., Ottosen, L.D.M., Nielsen, J.L., Kofoed, M.V.W., 2021. Cellulolytic and xylanolytic microbial communities associated with lignocellulose-rich wheat straw degradation in anaerobic digestion. Front. Microbiol. 12, 645174. https://doi.org/10.3389/fmicb.2021.645174.

Kaushal, R., Sandhu, S., Kumar Soni, M., 2022. Anaerobic co-digestion of food waste, algae, and cow dung for biogas yield enhancement as a prospective approach for environmental sustainability. Sustainable Energy Technol. Assess. 52, 102236. https://doi.org/10.1016/j.seta.2022.102236.

Kim, J.S., Lee, Y.Y., Kim, T.H., 2016. A review on alkaline pretreatment technology for bioconversion of lignocellulosic biomass. Bioresour. Technol. 199, 42–48. https://doi.org/10.1016/j.biortech.2015.08.085.

Kochi, L. Y., Freitas, P. L., Maranho, L. T., Juneau, P., & Gomes, M. P. (2020). Aquatic macrophytes in constructed wetlands: A fight against water pollution. In Sustainability (Switzerland) (Vol. 12, Issue 21, pp. 1–21). MDPI. doi: 10.3390/su12219202.

Li, Y., Merrettig-Bruns, U., Strauch, S., Kabasci, S., Chen, H., 2015. Optimization of ammonia pretreatment of wheat straw for biogas production. J. Chem. Technol. Biotechnol. 90 (1), 130–138. https://doi.org/10.1002/jctb.4297.

Liu, Y., Wu, Z., Lv, Y., Jiang, L., Wei, Y., Li, Y.Y., Liu, J., 2023. Recovery of an acidified food waste anaerobic digestion reactor via NH4+-N and trace metals addition: Performance, microbial community response, and mechanisms. J. Clean. Prod. 425, 138978. https://doi.org/10.1016/j.jclepro.2023.138978.

Louca, S., Parfrey, L.W., Doebeli, M., 2016. Decoupling function and taxonomy in the global ocean microbiome. Science 353 (6305), 1272–1277. https://doi.org/10.1126/science.aaf4507.

Luo, T., Huang, H., Mei, Z., Shen, F., Ge, Y., Hu, G., Meng, X., 2019. Hydrothermal pretreatment of rice straw at relatively lower temperature to improve biogas production via anaerobic digestion. Chin. Chem. Lett. 30, 1219–1223. https://doi.org/10.1016/j.cclet.2019.03.018.

Lymperatou, A., Engelsen, T.K., Skiadas, I.V., Gavala, H.N., 2022. Different pretreatments of beach-cast seaweed for biogas production. J. Clean. Prod. 362, 132277. https://doi.org/10.1016/j.jclepro.2022.132277.

Lymperatou, A., Gavala, H.N., Skiadas, I.V., 2017. Optimization of Aqueous Ammonia Soaking of manure fibers by Response Surface Methodology for unlocking the methane potential of swine manure. Bioresour. Technol. 244, 509–516. https://doi.org/10.1016/j.biortech.2017.07.147.

Mariotti, F., Tomé, D., Mirand, P.P., 2008. Converting nitrogen into protein - Beyond 6.25 and Jones' factors. Crit. Rev. Food Sci. Nutr. 48 (2), 177–184. https://doi.org/10.1080/10408390701279749.

Misson, G., Mainardis, M., Incerti, G., Goi, D., Peressotti, A., 2020. Preliminary evaluation of potential methane production from anaerobic digestion of beach-cast seagrass wrack: The case study of high-Adriatic coast. J. Clean. Prod. 254, 120131. https://doi.org/10.1016/j.jclepro.2020.120131.

Moeller, L., Bauer, A., Wedwitschka, H., Stinner, W., Zehnsdorf, A., 2018. Crop characteristics of aquatic macrophytes for use as a substrate in anaerobic digestion plants-a study from Germany. Energies 11 (11), 3016. https://doi.org/10.3390/en11113016.

Moiceanu, G., Paraschiv, G., Voicu, G., Dinca, M., Negoita, O., Chitoiu, M., Tudor, P., 2019. Energy Consumption at Size Reduction of Lignocellulose Biomass for Bioenergy. Sustainability 11 (9), 2477. https://doi.org/10.3390/su11092477.

Moussaoui, H., Chatir, K., Tuncer, A.D., Khanlari, A., Kouhila, M., Idlimam, A., Lamharrar, A., 2024. Improving environmental sustainability of food waste using a solar dryer: Analysing drying kinetics and biogas production potential. Sol. Energy 269, 112341. https://doi.org/10.1016/j.solener.2024.112341.

Nguyen, T.A.H., Bui, T.H., Guo, W.S., Ngo, H.H., 2023. Valorization of the aqueous phase from hydrothermal carbonization of different feedstocks: Challenges and perspectives. Chem. Eng. J. 472, 144802. https://doi.org/10.1016/j.cej.2023.144802.

Papastefanakis, N., Daliakopoulos, I.N., Maragkaki, A.E., Tsompanidis, C., Zotos, N., Lekkas, D.F., Manios, T., Fountoulakis, M.S., 2023. Application of solar drying as a pre-treatment method for storing wet feedstocks prior to use in anaerobic digesters: Effect on methane production and digestate composition. Fuel 348. https://doi.org/10.1016/j.fuel.2023.128477.

Perman, E., Schnürer, A., Björn, A., Moestedt, J., 2022. Serial anaerobic digestion improves protein degradation and biogas production from mixed food waste. Biomass Bioenergy 161, 106478. https://doi.org/10.1016/j.biombioe.2022.106478.

Poomsawat, S., Poomsawat, W., 2021. Analysis of hydrochar fuel characterization and combustion behavior derived from aquatic biomass via hydrothermal carbonization process. Case Stud. Therm. Eng. 27. https://doi.org/10.1016/j.csite.2021.101255.

Porras-Socias, P., Tomasino, M.P., Fernandes, J.P., De Menezes, A.B., Fernández, B., Collins, G., Alves, M.J., Castro, R., Gomes, C.R., Almeida, C.M.R., Mucha, A.P., 2024. Removal of metals and emergent contaminants from liquid digestates in constructed wetlands for agricultural reuse. Front. Microbiol. 15, 1388895. https://doi.org/10.3389/fmicb.2024.1388895.

Prenafeta-Boldú, F.X., Fernández, B., Viñas, M., Noguerol, J., Soler, J., Illa, J., 2021. Combined acidification and solar drying of pig slurries for nutrient recovery and controlled atmospheric emissions. Agronomy 11 (2), 222. https://doi.org/10.3390/agronomy11020222.

Ruiz-Sánchez, J., Campanaro, S., Guivernau, M., Fernández, B., Prenafeta-Boldú, F.X., 2018. Effect of ammonia on the active microbiome and metagenome from stable full-scale digesters. Bioresour. Technol. 250, 513–522. https://doi.org/10.1016/j.biortech.2017.11.068.

Struckmann Poulsen, J., de Jonge, N., Vieira Macêdo, W., Rask Dalby, F., Feilberg, A., Lund Nielsen, J., 2022. Characterisation of cellulose-degrading organisms in an anaerobic digester. Bioresour. Technol. 351, 126933. https://doi.org/10.1016/j.biortech.2022.126933.

Sun, H., Cui, X., Li, R., Guo, J., Dong, R., 2021. Ensiling process for efficient biogas production from lignocellulosic substrates: Methods, mechanisms, and measures. Bioresour. Technol. 342, 125928. https://doi.org/10.1016/j.biortech.2021.125928.

Thiemer, K., Schneider, S.C., Demars, B.O.L., 2021. Mechanical removal of macrophytes in freshwater ecosystems: Implications for ecosystem structure and function. Science of the Total Environment 782, 146671. https://doi.org/10.1016/j.scitotenv.2021.146671.

Usman, M., Shi, Z., Cai, Y., Zhang, S., Luo, G., 2023. Microbial insights towards understanding the role of hydrochar in enhancing phenol degradation in anaerobic digestion. Environ. Pollut. 330, 121779. https://doi.org/10.1016/j.envpol.2023.121779.

Vakalis, S., Georgiou, A., Moustakas, K., Fountoulakis, M., 2022. Assessing the effect of hydrothermal treatment on the volatile solids content and the biomethane potential of common reed (phragmites australis). Bioresour. Technol. Rep. 17. https://doi.org/10.1016/j.biteb.2021.100923.

Wang, H., Lim, T.T., Duong, C., Zhang, W., Xu, C., Yan, L., Mei, Z., Wang, W., 2020. Long-term mesophilic anaerobic co-digestion of swine manure with corn stover and microbial community analysis. Microorganisms 8, 188. https://doi.org/10.3390/microorganisms8020188.

Wang, L., Li, Y., Yi, X., Yang, F., Wang, D., Han, H., 2023. Dissimilatory manganese reduction facilitates synergistic cooperation of hydrolysis, acidogenesis, acetogenesis and methanogenesis via promoting microbial interaction during anaerobic digestion of waste activated sludge. Environ. Res. 218, 114992. https://doi.org/10.1016/j.envres.2022.114992.

Yang, Z., Wang, W., He, Y., Zhang, R., Liu, G., 2018. Effect of ammonia on methane production, methanogenesis pathway, microbial community and reactor performance under mesophilic and thermophilic conditions. Renew. Energy 125, 915–925. https://doi.org/10.1016/j.renene.2018.03.032.

Zwietering, M. H., Jongenburger, I., Rombouts, F. M., Van ' K., & Riet, T. (1990). Modelling of the bacterial growth curve. Applied and Environmental Microbiology, 56(6), 1875-1881. https://journals.asm.org/journal/aem.